© JUN 2026 | IRE Journals | Volume 9 Issue 12 | ISSN: 2456-8880
DOI: https://doi.org/10.64388/IREV9I12-1718753

Design and Evaluate Fire Sprinkler Mechanism Employing Shape Memory Alloy Technology Through Simulation

BATAO, JOHN LLOYD[1], MACALINTAL, DANICA JANE[2], OCAMPO, MHEEKA JOYCE[3]
[1,2,3]*Laguna University*

Abstract- ***A fire sprinkler system has to detect fire and actuate the sprinklers to discharge water automatically to put out the fire as soon as possible. Currently, when a fusible bulb fire sprinkler is exposed to fire, it opens and discharges water automatically but it is not able to stop the discharge of water when the fire is putout. This study presents the design and evaluation of a reusable fire sprinkler mechanism employing Shape Memory Alloy (SMA) technology through Finite Element Analysis (FEA). Unlike conventional sprinkler systems that use single-use glass bulbs or fusible links, the proposed mechanism utilizes SMA materials capable of automatic activation and reset through reversible phase transformation. Three SMA materials NiTi (Nitinol), NiTiNb, and Cu–Al–Ni were evaluated in terms of activation response time, actuation temperature behavior, generated force, stress distribution, deformation, and life-cycle performance under simulated fire conditions using ANSYS. Results showed that the SMA-based mechanism can automatically actuate during elevated temperatures and return to its original state after cooling, enabling reusable operation and reducing water wastage. Among the materials, NiTi exhibited faster response, NiTiNb demonstrated enhanced thermal stability, and Cu–Al–Ni showed suitability for high-temperature applications. The findings indicate that SMA-integrated sprinkler systems have strong potential for improving fire protection efficiency, reliability, and sustainability.***

Index Terms: ***Cu–Al–Ni Alloy, Fire Sprinkler Mechanism, NiTi (Nitinol), NiTiNb Alloy, Shape Memory Alloy (SMA)***

I. INTRODUCTION

This study focuses on the design and development of a Shape Memory Alloy (SMA)-based activation system for fire sprinkler applications using NiTinol, NiTiNb, and CuAlNi materials. Traditional fire sprinkler systems rely on fusible links or glass bulbs that respond to heat, but these components may have limitations in terms of response accuracy, reliability, and reusability. Shape Memory Alloys offer an alternative solution due to their ability to undergo phase transformation and return to a pre-defined shape when exposed to specific temperatures.

The research investigates the thermal and mechanical behavior of selected SMA materials under controlled heating conditions to determine their activation performance, particularly in terms of deflection and response time. Finite Element Analysis (FEA) is used to simulate the actuation behavior and compare the effectiveness of each material for sprinkler activation.

The results of this study aim to contribute to the improvement of fire sprinkler triggering mechanisms by identifying suitable SMA materials that can provide more efficient and reliable thermal activation.

II. LITERATURE REVIEW

Shape Memory Alloys in Engineering Applications: Shape Memory Alloys (SMAs) are smart materials that recover their original shape when exposed to heat due to phase transformation between martensite and austenite phases. Among these, Nitinol (NiTi) is most widely used due to its excellent superelasticity, fatigue resistance, and stable thermal response, making it suitable for actuator application [1]. The selection of SMAs depends on deformation and operating conditions to ensure reliable performance.

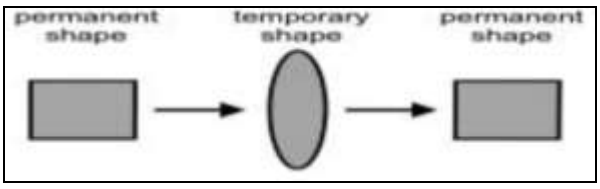

Figure 1. Simple Diagram Represents SMA Property

© JUN 2026 | IRE Journals | Volume 9 Issue 12 | ISSN: 2456-8880
DOI: https://doi.org/10.64388/IREV9I12-1718753

Fire Sprinkler Systems and Themal Activation: Fire sprinkler systems operates using heat-transitive elements such as glass bulbs or fusible alloys that activate at specific temperatures to release water for fire suppression [4]. According to NFPA 13 standards, these systems are designs for rapid response to heat buildup during fire incidents [5]. However,conventional thermal elements are typically single-use and may degrade over time, affecting long-term reliability[4].

SMA- Based Actuation Systems: SMAs have been explores as alternatives to traditional thermal triggers due to their ability to produce controlles mechanical motion when heat. SMA devices demonstrate reliable cyclic actuation behavior[6].The feasibilty of NiTinol-based sprinkler activation systems. These finding show that SMAs can enhance responsiveness and reduce maintenace requirements in fire protection.

Finite Element Analysis (FEA): Finite Element Analysis (FEA) is widely used to simulate the thermo-mechanical behavior of SMAs and predict deformation during phase transformation. [8][9]. According to study FEA is effective in evaluating SMA actuators in terms of displacement and response behavior,showing its applicability in real-life engineering systems and design evaluation.

Material Behavior of Niti, NiTiNb, and CuAlNi: NiTi exhibits stable actuation and hign recoverable strain under thermal loading [10]. NiTiNb is suitable for high-temperature applications due to improves therma stability and wides tranformation ranges [11]. CuAlNi provides very highetranformation temperatures and strong materials but show brittleness under cyclic loading [12]. These differences make each SMA suitable for specific thermal activation requirements.

Engineering Design Considerations: SMA actuator design requires integration of mechanical and thermal principles to ensure sufficient force and displacement for activation[13]. Proper mechaninical design ensures structural reliability under loading conditions, while SMA performance is influences by geometry and thermal input stability. [1]

III. METHODOLOGY

This study utilizes a simulation-based research design to evaluate the thermo-mechanical behavior of Shape Memory Alloy (SMA) materials—specifically Nitinol (NiTi), NiTiNb, and CuAlNi—for fire sprinkler activation applications. The analysis focuses on determining their suitability based on thermal response and mechanical deformation[14].

Material properties, including transformation temperature, elastic modulus, and thermal characteristics, were obtained from published literature and used as input parameters for the simulation model. A finite element analysis (FEA) approach was then employed to simulate the actuation behavior of each SMA under uniform thermal loading conditions.[15]

All materials were evaluated using the same geometric setup and boundary conditions to ensure consistent comparison. The results were analyzed in terms of displacement, stress distribution, and response behavior to identify the most effective SMA for thermal activation systems.[9]

Table 1. Physical Properties of SMA (Austenite)

Mechanical Properties	Austenite		
	NiTinol	NiTINb	CuAlNi
Coefficient of Thermal Expansion	1.1×10^{-6}	1.2×10^{-7}	I. 1.7×10^{-7}INTRODUCTION
Density	6700 kg/m³	6700 kg/m³	7100 kg/m³
Young's Modulus	8.3×10^{10}Pa	9×10^{10} Pa	8×10^{10}Pa
Poisson's Ratio	0.33	0.28571	0.34
Bulk Modulus	8.1373×10^{10} Pa	7×10^{10} Pa	8.3333×10^{10} Pa
Shear Modulus	3.1203×10^{10} Pa	3.5×10^{10} Pa	2.9851×10^{10} Pa

© JUN 2026 | IRE Journals | Volume 9 Issue 12 | ISSN: 2456-8880
DOI: https://doi.org/10.64388/IREV9I12-1718753

Table 2. Physical Properties of SMA (Martensite)

Mechanical Properties	Austenite		
	NiTinol	NiTINb	CuAlNi
Coefficient of Thermal Expansion	6.6×10^{-6}	8×10^{-6}	1.2×10^{-7}
Density	6450 kg/m³	6450 kg/m³	7100 kg/m³
Young's Modulus	4.1×10^{10}Pa	5×10^{10}Pa	4×10^{10}Pa
Poisson's Ratio	0.33	0.25	0.34
Bulk Modulus	4.0196×10^{10} Pa	3.333×10^{10} Pa	4.1667×10^{10} Pa
Shear Modulus	1.54×10^{10} Pa	2×10^{10} Pa	1.4925×10^{10} Pa

Table 3. Thermal Properties of SMA (Austenite)

Thermal Properties	Austenite		
	NiTinol	NiTiNb	CuAlNi
Hardening Parameter	9×10^{8} Pa	1×10^{9} Pa	8.2×10^{8} Pa
Elastic Limit	5.5×10^{8} Pa	6×10^{8} Pa	2×10^{8} Pa
Temperature Scaling	9×10^{5} Pa	1×10^{6} Pa	1×10^{4} Pa
Maximum Trasformation Strain	0.06mm	0.08mm	0.06mm
Martensite Modulus	8×10^{10} Pa	5×10^{10} Pa	9×10^{10} Pa
Thermal Conductivity	10W/m·C	12W/m·C	43W/m·C
Specific Heat	322 J/kg-C	400 J/kg-C	500 J/kg-C

Proposed Model: Two actuator configurations were developed in the study: the vertical configuration and the horizontal configuration. Each design consisted of five major components including the main chamber, SMA spring actuator, piston, spring chamber, and gasket assembly. The SMA Spring served as the primary thermal activation component responsible for initiating sprinkler actuation during elevated temperature conditions.

Design 1
Horizontal Configuration Design

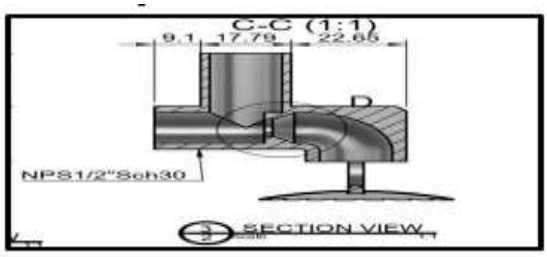

Figure 2. Section View Of Horizontal Design of Innovative SMA Fire Sprinkler

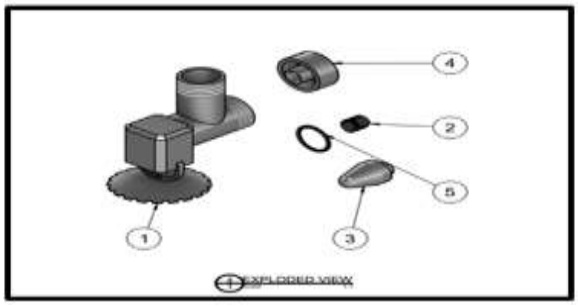

Figure 3.Exploded View Horizontal Design Of Innovative SMA Fire Sprinkler Assembly

Contruction: Figure 2 displays the Exploded View of the Horizontal Design of Innovative SMA Fire Sprinkler, detailing the assembly of its five core components. The Main Chamber (1) connects to the internal actuation mechanism comprising the SMA Spring (2), Piston (3), and Gasket (5) which are secured within the Spring Chamber (4). This view provides the structural basis for the comparative analysis between theoretical calculations and simulation results.

Design 2
Vertical Configuration Design

© JUN 2026 | IRE Journals | Volume 9 Issue 12 | ISSN: 2456-8880
DOI: https://doi.org/10.64388/IREV9I12-1718753

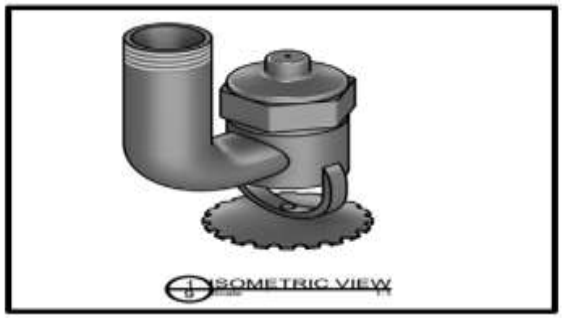

FIGURE 4. Isometric View of Vertical Design of Innovative SMA Fire Sprinkler

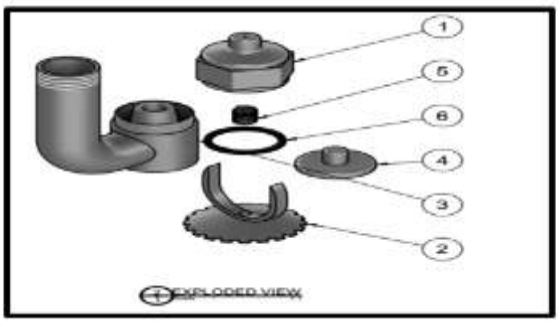

Figure 5. Exploded View of Isometric View of Vertical Design of Innovative SMA Fire Sprinkler

Figure 5 displays the Exploded View of the Innovative SMA Fire Sprinkler, detailing the assembly of its five core components. The Main Chamber (1) connects to the internal actuation mechanism comprising the SMA Spring (2), Piston (3), and Gasket (5) which are secured within the Spring Chamber (4).

Parameter formula: The mechanical behavior of Shape Memory Alloy (SMA) spring actuators was evaluated using fundamental spring mechanics and stress analysis equations. These equations were applied to determine stiffness, deformation, stress distribution, strain behavior, safety factor, and fatigue life under applied loading conditions. The spring mechanics equations used in this study were adopted from the book Design of Machine Elements, 4th Edition by Virgil M. Faires, pages 183–188.[16]

The stiffness of the helical spring is determined using:

$$\kappa=\frac{Gd^4}{8D^3n} \quad (1)$$

where, κ is the spring stiffness, G is the shear modulus, d is the wire diameter, D is the mean coil diameter, and nnn is the number of active coils.

The spring deflection is calculated using :

$$\delta=\frac{8FD^3n}{Gd^4} \quad (2)$$

where, δ is the spring deflection and "F " is the applied force.
The shear stress in the spring wire is determined using:

$$\tau=\frac{K_w\,8FD}{\pi d^3} \quad (3)$$

where, τ is the shear stress and Kw is the Wahl correction factor given in Eq. (4).'

$$K_W=\frac{4C-1}{4C-4}+\frac{0.615}{C} \quad (4)$$

The shear strain is calculated using:

$$Y=\frac{\tau}{G} \quad (5)$$

The equivalent Von Mises stress used for yielding prediction is expressed in:

$$\sigma_{vm}=\sqrt{\sigma_n^2+3\tau^2} \quad (6)$$

The factor of safety is determined using:

$$N=\frac{S_y}{\sigma_{vm}} \quad (7)$$

where, Sy is the yield strength of the material.

Hooke's Law relating force and deflection is expressed in:

$$F=\delta\kappa \quad (8)$$

The recoverable elastic strain is determined using:

$$\varepsilon_{elastic}=\frac{\delta}{Lo} \quad (9)$$

The equivalent strain used in FEA is calculated using:

$$\varepsilon=\frac{\tau}{G_{eff}\sqrt{3}} \quad (10)$$

The applied force is determined using:

$$F=P\times A \quad (11)$$

Finite Element Analysis

Table 4. Mesh Statistics

MATERIALS	Horizontal/Vertical		
	Nitinol	NitiNb	CuAlNi
Number Of Elements	27125	27125	101688
Number Of Nodes	131360	131360	443693
Elements Size	0.1 mm	0.1 mm	0.1 mm
Mesh Type	Quad/tri	Quad/tri	Quad/tri

The mesh density varied according to the geometry and complexity of each actuator configuration. Vertical models contained more elements and nodes than horizontal models due to their more complex structure and loading conditions.

A fine mesh size of 1.0×10−4 m was applied to most models to accurately capture stress concentration and deformation behavior, while the Cu–Al–Ni horizontal model used a slightly modified mesh size because of geometric and meshing constraints. A hybrid Quad/Tri mesh was employed to balance meshing flexibility and computational efficiency. Mesh quality verification and refinement confirmed solution convergence, as further increases in mesh density produced no significant changes in the simulation results.

Finite Element Analysis (FEA) was conducted using ANSYS 2024 R1 under controlled thermal loading conditions from ambient room temperature (31°C)[17], the highest recorded ambient heat condition in the Philippines (42°C)[18], and high-hazard fire exposure temperature (149°C), up to approximately 191°C [19], with a fixed simulation time of 10 seconds to evaluate activation response time and an applied internal pressure of 10 psi to simulate operating conditions[19]. These temperature conditions were incorporated to determine the thermal behavior and activation response of the Shape Memory Alloy (SMA) materials under normal, extreme ambient, and fire hazard environments.

The model was evaluated in terms of displacement, stress distribution, recoverable strain, and thermal activation behavior, with identical geometry and boundary conditions applied across all cases to ensure consistent comparison. The results were validated using theoretical calculations based on spring mechanics and strength of materials, including shear stress, deflection, equivalent stress, and factor of safety. Finally, the SMA materials and configurations were assessed in terms of activation temperature, actuation displacement, recovery force, fatigue behavior, and structural stability, with consideration of National Fire Protection Association standards under NFPA 13 and the Fire Code of the Philippines (RA 9514) to determine the most suitable SMA-based actuator for fire sprinkler applications.

Comparative Evaluation of SMA Materials: The SMA materials and actuator configurations were comparatively analyzed based on activation response time, activation temperature, displacement behavior, stress distribution, thermal recovery capability, fatigue resistance, and structural stability. The results obtained from theoretical calculations and FEA simulations were compared to determine the most suitable SMA material for reusable fire sprinkler applications.

Standards and Design Considerations:The proposed SMA-based fire sprinkler mechanism was evaluated with consideration to the requirements of NFPA 13: Standard for the Installation of Sprinkler Systems and the Fire Code of the Philippines (Republic Act No. 9514). These standards were considered to ensure the suitability, reliability, and operational effectiveness of the proposed mechanism for fire protection applications.

© JUN 2026 | IRE Journals | Volume 9 Issue 12 | ISSN: 2456-8880
DOI: https://doi.org/10.64388/IREV9I12-1718753

IV. RESULTS

Theoretical Vs. Simulation Results. To evaluate the agreement between the theoretical calculations and ANSYS simulation results, the percent difference was calculated using:

$$\text{Percent (\%) Difference} = \frac{\text{Theoretical Values - Simulation Results}}{\text{Theoretical Value}}$$

The comparison shows a strong correlation between the theoretical and simulated results for both horizontal and vertical actuator designs. Parameters such as deformation, stress, and generated force exhibited only minimal variation. All computed percent differences were less than 5%, validating the accuracy and reliability of the ANSYS Finite Element Analysis (FEA) model. Slight variations are attributed to differences between ideal theoretical assumptions and the realistic conditions considered in the simulation, including mesh discretization, boundary conditions, and stress concentrations.

Activation Response Time of SMA. Figure 7 show that NiTi showed the fastest activation response, reaching 2.41 mm deflection in 4.667 s at 68 °C. NiTiNb activated more slowly at 6.53 s and 120 °C, indicating better thermal stability. CuAlNi failed to reach the required activation deflection, resulting in an undetermined response time. Overall, NiTi exhibited the best activation performance among the tested SMA materials.

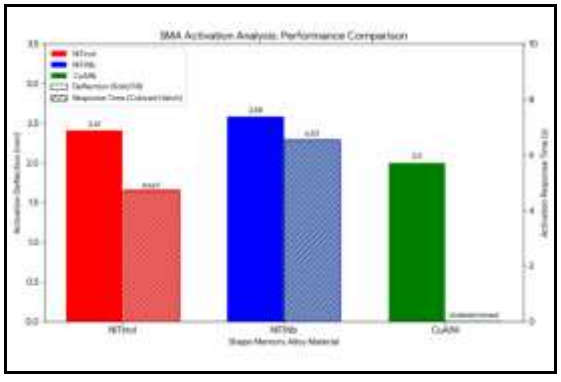

Figure 6. Activation Response Time of SMA Analysis Performance

Life Cycle Performance of SMA.The life cycle performance was determined using the S–N (Stress–Number of Cycles) curve obtained from ANSYS fatigue analysis. The S–N curve relates the applied stress level to the number of cycles the material can withstand before failure. Based on the simulated stress results, CuAlNi exhibited the highest life cycle performance with 1.0×109 cycles, indicating superior durability under repeated thermal loading. In comparison, both NiTi and NiTiNb demonstrated life cycles of 1.0×107 cycles, showing high fatigue resistance and stable cyclic behavior. Although CuAlNi had the greatest durability, NiTi and NiTiNb provided a more balanced performance due to their faster activation response and reliable actuation capability.

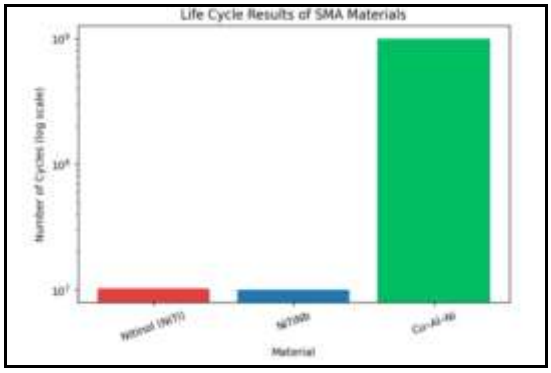

Figure 7. Life Cycle Performance of SMA

Equivalent (Von Misses) Stress Analysis of SMA. The stress analysis was determined using Finite Element Analysis (FEA) based on the equivalent (von Mises) stress distribution of the SMA actuators under thermal and mechanical loading conditions. Figure 9 shows the results showed that NiTi and NiTiNb exhibited higher stress values of 169.41 MPa and 167.79 MPa, respectively, indicating stronger recovery forces during phase transformation. In contrast, CuAlNi produced the lowest stress value of 54.519 MPa, indicating lower internal mechanical loading and more uniform stress distribution. Despite the differences in stress magnitude, all materials remained within safe structural limits, confirming stable mechanical performance and structural integrity during operation.

© JUN 2026 | IRE Journals | Volume 9 Issue 12 | ISSN: 2456-8880
DOI: https://doi.org/10.64388/IREV9I12-1718753

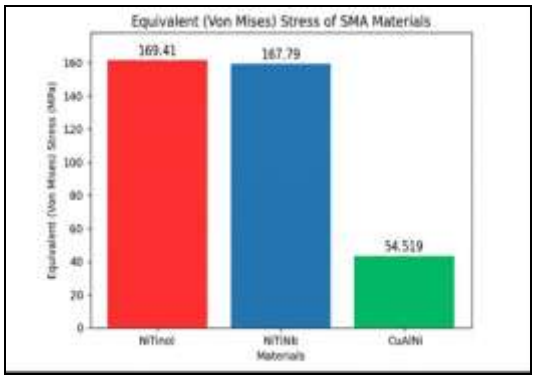

Figure 8. Equivalent (Von Mises) Stress of SMA

Temperature Behavior of SMA. Figure 9 presents the activation temperature behavior and deformation response of the three SMA materials—NiTi, NiTiNb, and Cu–Al–Ni—based on NFPA 13 classification ranges. The results show that all materials exhibit minimal deformation at low temperatures (31 °C and 42 °C), while significant actuation occurs at 149 °C due to phase transformation. NiTi demonstrates the highest deformation 5.1702 mm and aligns with the ordinary temperature range, indicating strong and efficient actuation. NiTiNb shows moderate deformation 4.4404 mm with high-temperature classification behavior, while Cu–Al–Ni exhibits the lowest response 0.64435 mm, indicating weak actuation performance. Overall, the figure highlights that NiTi provides the most effective thermal activation response for SMA-based fire sprinkler applications under NFPA 13

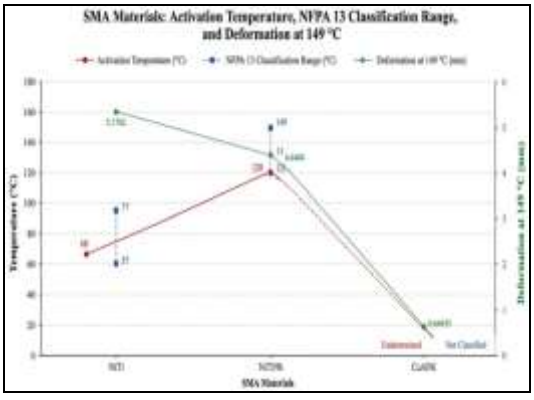

Figure 9. Activation Temperature, NFPA 13 Classification Range, and Deformation at 149°C

Total Generated Force of Vertical and Horizontal SMA.The simulation results in figure 10 showed that both vertical and horizontal configurations produced comparable generated force and total deformation responses among the tested SMA materials. For generated force, Cu–Al–Ni exhibited the highest force output in both configurations, producing 0.87195 N in the vertical configuration and 0.8711 N in the horizontal configuration. Meanwhile, Nitinol and NiTiNb generated lower but nearly identical force values ranging from 0.375 N to 0.377 N. In terms of total deformation, Nitinol demonstrated the highest deformation response with 5.1702 mm in the vertical configuration and 5.1600 mm in the horizontal configuration. However, the excessive deformation caused the Nitinol sprinkler mechanism to bend under thermal loading conditions, which may affect the structural stability and performance of the fire sprinkler mechanism. NiTiNb produced moderate deformation values of 4.4404 mm and 4.5437 mm, while Cu–Al–Ni showed the lowest deformation with 0.64435 mm and 0.81848 mm. Overall, the results indicate that Cu–Al–Ni generated the highest force output, while Nitinol exhibited the greatest deformation but experienced bending behavior that could negatively affect sprinkler performance.

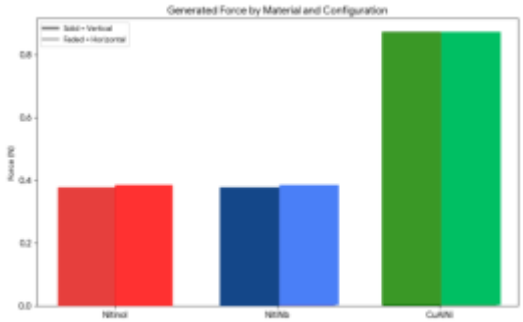

Figure 10. Generated Force of Vertical and Horizontal SMA

Life Cycle Performance for Vertical and Horizontal SMA.

Table 5. Life Cycle Performance of Vertical Configuration SMA

Configuration	Vertical		
Materials	Nitinol	NitiNb	CuAlNi
Life Cycle (Cycles)	10^7	10^7	10^9

Recoverable Strain(%)	75.8%	59.6%	10.7%

Table 6. Life Cycle Performance of Horizontal Configuration

Configuration	Vertical		
Materials	Nitinol	NitiNb	CuAlNi
Life Cycle (Cycles)	10^7	10^7	10^9
Recoverable Strain(%)	75.8%	59.6%	10.7%

The simulation results showed that both vertical and horizontal configurations produced comparable generated force and total deformation responses among the tested SMA materials. For generated force, Cu–Al–Ni exhibited the highest force output in both configurations, producing 0.87195 N in the vertical configuration and 0.8711 N in the horizontal configuration. Meanwhile, Nitinol and NiTiNb generated lower but nearly identical force values ranging from 0.375 N to 0.377 N. In terms of total deformation, Nitinol demonstrated the highest deformation response with 5.1702 mm in the vertical configuration and 5.1600 mm in the horizontal configuration. However, the excessive deformation caused the Nitinol sprinkler mechanism to bend under thermal loading conditions, which may affect the structural stability and performance of the fire sprinkler mechanism. NiTiNb produced moderate deformation values of 4.4404 mm and 4.5437 mm, while Cu–Al–Ni showed the lowest deformation with 0.64435 mm and 0.81848 mm. Overall, the results indicate that Cu–Al–Ni generated the highest force output, while Nitinol exhibited the greatest deformation but experienced bending behavior that could negatively affect sprinkler performance.

Factor of Safety of Vertical and Horizontal Configuration SMA.The Factor of Safety (FoS) results showed in figure 11 for the SMA materials under both configurations show that Cu–Al–Ni has the highest FoS values (7.3369–7.2806), indicating the greatest structural safety margin. NiTi exhibits FoS values of 2.4498–2.4435, while NiTiNb shows slightly lower values of 2.3840–2.3776.

The minimal variation between vertical and horizontal configurations suggests that orientation has negligible influence on structural safety performance. Although Cu–Al–Ni provides the highest safety margin, its low deformation response limits its suitability for actuator applications compared to NiTi-based alloys.

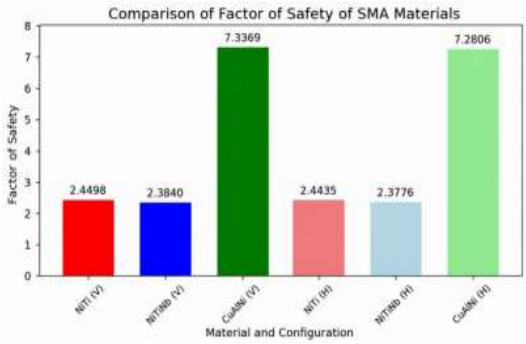

Figure 11. Results of Factor of Safety of Vertical and Horizontal Configuration SMA

V. CONCLUSIONS

The Shape Memory Alloy (SMA)-Based Fire Sprinkler Mechanism was successfully conceptualized, designed, and evaluated through simulation using Finite Element Analysis (FEA). The study demonstrates the feasibility of integrating SMA materials (NiTi, NiTiNb, and Cu–Al–Ni) into a reusable fire sprinkler system capable of thermally induced actuation and recovery. The developed system addresses the limitations of conventional single-use sprinkler mechanisms by introducing a resettable and thermally responsive alternative.

Key outcomes of the study include:

Effective Thermal Activation Behavior.
All SMA materials exhibited minimal deformation at 31 °C and 42 °C, while significant actuation occurred at 149 °C due to phase transformation. NiTi produced the highest deformation (5.1702 mm), followed by NiTiNb (4.4404 mm), while Cu–Al–Ni showed the lowest response (0.64435 mm), confirming temperature-dependent activation performance.

Superior Actuation Performance of NiTi.
Among the tested materials, NiTi demonstrated the fastest activation response and the highest

recoverable strain. NiTi achieved a recoverable strain of 75.80%–75.93%, indicating strong shape recovery capability under thermal loading. NiTiNb exhibited moderate performance with improved thermal stability, while Cu–Al–Ni showed limited actuation capability under identical conditions.

The recoverable strain was computed as the ratio of total deformation to the original length of the SMA actuator ($\varepsilon = \delta / L_o$).

Structural Safety and Stability.
Factor of safety analysis revealed that Cu–Al–Ni obtained the highest safety margin (7.3369–7.2806), followed by NiTi (2.4498–2.4435) and NiTiNb (2.3840–2.3776). All materials remained within safe design limits under both vertical and horizontal configurations, confirming structural reliability.

Fatigue and Life Cycle Performance.
NiTi and NiTiNb both achieved a life cycle of 10^7 cycles, while Cu–Al–Ni reached 10^9 cycles, indicating superior fatigue resistance. However, Cu–Al–Ni's low recoverable strain (10.7%) limits its effectiveness for actuation-based applications.

Configuration Consistency.
Both vertical and horizontal configurations showed minimal differences in deformation, stress, and safety performance, indicating that actuator orientation has negligible effect on system behavior.

Overall System Performance.
The results confirm that SMA-based technology is a viable solution for reusable fire sprinkler systems. Among the materials evaluated, NiTiNb provides the most balanced performance in terms of actuation response, deformation capability, and recoverable strain, making it the most suitable material for fire sprinkler activation applications.

REFERENCES

[1] National Fire Sprinkler Association, "Types of Fire Sprinkler Systems," 2019.

[2] J. Hu, "Investigation on the cyclic response of superelastic shape memory alloy slit damper devices," Materials, vol. 7, no. 2, pp. 1122–1141, 2014.

[3] V. M. Dornelas et al., "Numerical investigations of shape memory alloy fatigue," Metals, vol. 11, no. 10, p. 1558, 2021.

[4] X. Gao et al., "Finite element analysis of adaptive-stiffening and shape-control SMA hybrid composites," Journal of Engineering Materials and Technology, vol. 128, no. 3, pp. 285–293, 2006.

[5] H. Llewellyn-Evans et al., "Design process and simulation testing of a shape memory alloy actuated robotic microgripper," Microsystem Technologies, vol. 26, pp. 885–900, 2019.

[6] G. K. Tshikwand et al., "Coupled finite element simulation of shape memory bending microactuator," Shape Memory and Superelasticity, vol. 8, no. 4, pp. 373–393, 2022.

[7] L. Xu et al., "Finite strain constitutive modeling for shape memory alloys," arXiv preprint, 2020.

[8] V. Ziavras, "Sprinkler system basics: Types of sprinkler systems," NFPA, 2021.

[9] W. Huang, "On the selection of shape memory alloys for actuators," Materials & Design, vol. 23, no. 1, pp. 11–19, 2002.

[10] C. Lin et al., "Experimental study on temperature effects on NiTi shape memory alloys," Materials, vol. 13, no. 3, p. 573, 2020.

[11] C. Ying et al., "Mechanical behavior in NiTiNb shape memory alloys," Intermetallics, vol. 19, no. 2, pp. 217–220.

[12] V. Pushin et al., "Mechanical behavior and structural characterization of a Cu–Al–Ni shape-memory alloy," Materials, vol. 15, p. 3713, 2022.

[13] E. Tachibana et al., "Finite element analysis for shape memory alloy," 1986.

[14] D. C. Lagoudas, Shape Memory Alloys: Modeling and Engineering Applications. New York, USA: Springer, 2008.

[15] ANSYS Inc., ANSYS Mechanical APDL Theory Reference, Release 2024 R1, Canonsburg, PA, USA, 2024.

[16] .V. M. Faires and J. E. Shames, Design of Machine Elements, 4th ed. New York, USA: Macmillan Publishing Co., 1970, pp. 183–188.

[17] Philippine Atmospheric, Geophysical and Astronomical Services Administration (PAGASA), “Daily Temperature Monitoring Report,” 2026.

[18] PAGASA heat index report, “Metro Manila and several areas recorded danger-level heat indices ranging from 42°C to 46°C,” 2025

[19] National Fire Protection Association, NFPA 13: Standard for the Installation of Sprinkler Systems, 2022 ed., Quincy, MA, USA, 2022.